TERM

ORIGINAL ARTICLE

Preparation and *In Vitro* Characterization of Gelatin Methacrylate for Corneal Tissue Engineering

Yayun Yan[1] · Yanyan Cao[1,2] · Rong Cheng[1] · Zhizhong Shen[1] · Yajing Zhao[1] ·
Yixia Zhang[3] · Guohong Zhou[4] · Shengbo Sang[1]

Abstract

BACKGROUND: Corneal disease is second only to cataract considered as the leading cause of blindness in the world, with high morbidity. Construction of corneal substitutes *in vitro* by tissue engineering technology to achieve corneal regeneration has become a research hotspot in recent years. We conducted in-depth research on the biocompatibility, physicochemical and mechanical properties of rat bone marrow mesenchymal stem cells (rBM-MSCs)-seeded gelatin methacrylate (GelMA) as a bioengineered cornea.

METHODS: Four kinds of GelMA with different concentrations (7, 10, 15 and 30%) were prepared, and their physicchemical, optical properties, and biocompatibility with rBM-MSCs were characterized. MTT, live/dead staining, cell morphology, immunofluorescence staining and gene expression of keratocyte markers were performed.

RESULTS: 7%GelMA hydrogel had higher equilibrium water content and porosity, better optical properties and hydrophilicity. In addition, it is more beneficial to the growth and proliferation of rBM-MSCs. However, the 30%GelMA hydrogel had the best mechanical properties, and could be more conducive to promote the differentiation of rBM-MSCs into keratocyte-like cells.

CONCLUSION: As a natural biological scaffold, GelMA hydrogel has good biocompatibility. And it has the ability to promote the differentiation of rBM-MSCs into keratocyte-like cells, which laid a theoretical and experimental foundation for further tissue-engineered corneal stromal transplantation, and provided a new idea for the source of seeded cells in corneal tissue engineering.

Keywords Bioengineered cornea · Bone marrow mesenchymal stem cells · Corneal tissue engineering · Gelatin methacrylate · Hydrogel

✉ Shengbo Sang
sunboa-sang@tyut.edu.cn

1 MicroNano System Research Center, College of Information and Computer & Key Lab of Advanced Transducers and Intelligent Control System, Ministry of Education, Taiyuan University of Technology, Taiyuan 030024, China

2 College of Information Science and Engineering, Hebei North University, Zhangjiakou 075000, China

3 College of Biomedical Engineering, Taiyuan University of Technology, Taiyuan 030024, China

4 Department of Lacrimal Duct Diseases, Shanxi Eye Hospital, Taiyuan 030002, China

1 Introduction

The thickness of corneal tissue is about 500 μm, which is composed of three different cell types (epithelial cells, stromal cells and endothelial cells) and three layers (epithelial layer, stromal layer and endothelial layer). The cornea is a transparent film located at the forefront of the eyeball. It is an important protective barrier for the eyeball and an important part of the eyeball optical system, which determines the clarity of vision [1, 2]. Many factors, such as mechanical, thermal, chemical damage and microbial infections, can cause the transparent cornea to appear

grayish and cloudy, and may even lead to vision loss and blindness [3]. This physiological phenomenon is known as corneal disease, which is second only to cataract considered as the leading cause of blindness in the world, with high morbidity. At present, about 20 million people worldwide are blinded by corneal diseases [4]. Allogeneic corneal transplantation is the most effective method to treat corneal diseases, but it is difficult to achieve good curative effects and meet increasing medical needs, due to the lack of donors, immune rejection or biocompatibility, infection and other problems. The appearance of corneal tissue engineering brings happiness and hope for treating and preventing corneal lesions [5–11].

Many kinds of scaffolds materials can be used for corneal tissue engineering, including porcine cornea, collagen, silk film, chitosan, biodegradable synthetic polymers and composite materials [12–16]. Hydrogels can swell in water or biological fluids and retain large amounts of water without being dissolved. The structure of hydrogels is similar to human tissues and does not affect the metabolic process of organisms. Metabolites can be discharged smoothly, so hydrogels are often used as substitutes for human organs/tissues. Hayes et al. synthesized a corneal substitute using recombinant human type III collagen [17]. Lawrence et al. prepared biomimetic corneal matrix tissue using silk protein membrane as scaffold material [18]. As the main component of the extracellular matrix (ECM), collagen has perfect biocompatibility and biodegradability, which is beneficial to promote regeneration of active progenitor cells and can be used as a natural biomaterial for corneal replacement [19]. However, one of the difficulties of natural collagen is its poor mechanical properties, which usually results in excessive deformation due to the contraction behavior of cells. Besides, Stafiej et al. evaluated the adhesion and metabolic activity of human corneal cells based on polycaprolactone (PCL) nanofiber matrix [20]. The disadvantage of PCL is that it is not easily degraded after implantation. Corneal-derived acellular extracellular matrix has also been used in corneal research, but its low yield and immunogenicity also make it have certain limitations [21].

Collagen is abundant in the human body, while gelatin is a protein mixture produced by acid or alkaline hydrolysis of collagen. The chemical composition of gelatin is similar to collagen, which is widely used in pharmaceutical, food, cosmetics and other fields [22]. As a biodegradable material, gelatin has good tissue compatibility and can be degraded naturally *in vivo* without causing tissue inflammation. Linear polymer formed by cross-linking of amino acids and peptide chains can undergo a variety of surface modifications and reactions. In addition, materials containing the RGD sequence can increase cell adhesion [23, 24]. In recent years, a new type of photosensitive hydrogel [Gelatin methacrylate (GelMA)] has been widely favored by scholars. GelMA is prepared by graft modification. The presence of methacrylic anhydride group makes it photosensitive and can be cross-linked rapidly under ultraviolet (UV, 365 nm) or near-UV blue light (405 nm). Cell-loaded GelMA hydrogels have been widely used in a variety of tissue-engineering applications because GelMA can precisely adjust the properties of the hydrogel by changing the conditions during its synthesis to suit the target tissue and ensure cell survival [25, 26]. At the same time, GelMA also has good biodegradability and excellent biocompatibility. Farasatkia et al. used silk nanofibrils and GelMA in corneal tissue engineering to obtain composites with good mechanical, optical and biological properties [27]. Bektas et al. applied cell-loaded GelMA hydrogels of and poly(2-hydroxyethyl methacrylate) to corneal tissue engineering. Cells synthesized representative collagens and proteoglycans in the hydrogels indicating that they preserved their keratocyte functions [28].

Stem cell research has brought hope for the treatment of many diseases and injuries [29]. In particular, the application of pluripotent adult stem cells has attracted extensive attention because it does not involve ethical issues. A lot of researches have shown that bone marrow mesenchymal stem cells (BM-MSCs) have been used in corneal tissue engineering [19]. Carter et al. conducted the study of *in vitro* corneal wound healing using BM-MSCs to facilitate faster corneal wounds healing [30]. Studies have investigated and verified the efficacy of BM-MSCs and adipose tissue-derived mesenchymal stem cell in corneal wound healing [31, 32]. Rohaina et al. also confirmed that BM-MSCs could be used in the limbal stem cell deficient model to achieve the reconstruction of the corneal surface [33].

In this study, we used methacrylic anhydride (MA) to modify gelatin to prepare GelMA that can be polymerized by near-UV blue light ($\sim$ 405 nm) to initiate free radical polymerization. The physic-chemical characterization of GelMA hydrogels were evaluated. In particular, rat bone marrow mesenchymal stem cells (rBM-MSCs) were used to assess the biocompatibility of GelMA hydrogels in various concentrations. The ability of rBM-MSCs to differentiate into keratocyte-like cells was characterized by immunofluorescence staining and gene expression of keratocyte markers, including Keratocan, Lumican, ALDH1A1, α-SMA. Our study verified that 30%GelMA hydrogel could provide a better dynamic microenvironment for rBM-MSCs to differentiate into keratocyte-like cells**.**

2 Materials and methods

2.1 Materials

Gelatin powder (type A gelatin derived from porcine skin), L-ascorbic-acid-2-phosphate and amphotericin B were purchased from Sigma-Aldrich. MA, lithium phenyl(2,4,6-trimethylbenzoyl) phosphate (LAP), penicillin, streptomycin, penicillin/streptomycin, methyl thiazolyl tetrazolium (MTT) and dimethylsulfoxide (DMSO) were obtained from Macklin. Dulbecco's Modified Eagle Medium and Ham's Nutrient Mixture F-12 (DMEM/F12), fetal bovine serum (FBS) and Dulbecco's Modified Eagle Medium (DMEM) were purchased from Thermo Fisher Scientific. Phalloidin was acquired from Abbkine. Live-dead assay kit was provided from BestBio. GlutaMAX^{TM} was purchased from Gibco. 4',6-dimidyl-2-phenylindole (DAPI) was obtained from Boster. cDNA synthesis kit and SYBR Premix Ex Taq were acquired from Juhemei. Anti-Lumican and FITC-labeled goat anti-rabbit IgG were provided from Abcam.

2.2 Preparation of GelMA

GelMA was synthesized by grafting modification as described previously (Fig. 1) [34]. Briefly, the mixture of 5 g of gelatin and 50 mL of phosphate buffered saline (PBS) was stirred until completely dissolved at 60 °C. And 4 mL of MA was slowly added to the gelatin solution, and the mixture was reacted for 3 h at 50 °C. Then 200 mL PBS was added for dilution to terminate the reaction at 40 °C. To remove salt and MA, 14 kDa cutoff dialysis bag was used to dialysis the mixture for 1 or 2 weeks. Finally, GelMA was prepared by lyophilizing the mixture and stored at −80 °C.

A certain amount of lyophilized GelMA was dissolved in PBS at 37 °C, and LAP (0.25% w/v) was added as a photoinitiator to form prepolymer solutions of different concentrations (7, 10, 15 and 30% (w/v)). The GelMA hydrogel was prepared by crosslinking the prepolymer solution under near-UV blue light (~ 405 nm) for 30 s to evaluate its mechanical properties, contact angle, optical properties and biodegradability. The prepolymer solution was sterilized by filtration with 0.22 μm filter before cell experiments. rBM-MSCs were seeded on the surface of the hydrogel at a density of 1×10^4 cells/cm^2.

2.3 Fourier transform infrared spectroscopy (FTIR)

Potassium Bromide pressed-disk technique was used to evaluate FTIR of gelatin, GelMA and GelMA hydrogel by Fourier infrared spectrometer (Bruker, ALPHAII, Melle, Germany). Briefly, the gelatin, GelMA, GelMA hydrogel and KBr were mixed (1: 100) respectively for FTIR analysis after compression [19].

2.4 Scanning electron microscope (SEM) and porosity

The GelMA hydrogel was prepared according to the above method and freeze-dried. SEM (JEOL, Japan) with acceleration voltage of 5 kV was used to evaluate the internal morphology of the GelMA hydrogel. In addition, Archimedes' principle was used to evaluate the porosity of freeze-dried GelMA hydrogels. Briefly, freeze-dried GelMA hydrogel (W_4) was placed into a bottle full of ethanol (W_1). The weight of the bottle with ethanol and GelMA hydrogel after 24 h immersion was recorded as W_2. After removing GelMA, the weight of the bottle with ethanol was recorded as W_3. Then, the porosity was calculated by the following formula [19]:

$$\text{porosity(wt.-\%)} = \frac{W_2 - W_3 - W_4}{W_1 - W_3} \times 100\% \tag{1}$$

2.5 Equilibrium water content and degradation

The GelMA hydrogels was placed in PBS (pH = 7.4) at 37 °C and immersed completely to characterize equilibrium water content. After 48 h, the GelMA hydrogel was removed from the PBS and excess water on the surface of
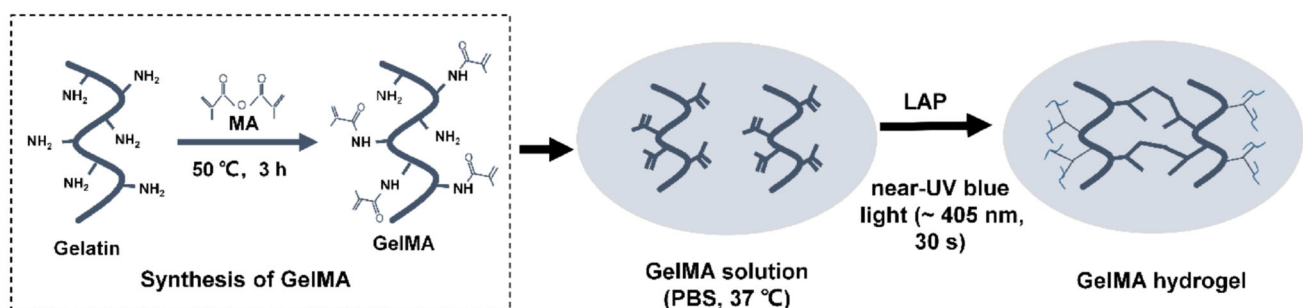

Fig. 1 Synthesis of gelatin methacrylate (GelMA) hydrogel

the GelMA hydrogel was removed by filter paper. The equilibrium water content of GelMA hydrogels (W_e) was calculated by the following formula:

$$W_e(\text{wt.-\%}) = \frac{W_w - W_d}{W_w} \times 100\% \quad (2)$$

In the formula above, W_d and W_w are the weight of the GelMA hydrogels before and after being immersed in PBS, respectively.

The degradation behavior of hydrogel *in vitro* is an important factor affecting the development of corneal tissue engineering [35]. Four kinds of GelMA hydrogels with different concentrations (7, 10, 15 and 30%) were evaluated in PBS at pH 7.4 and 37 °C for an *in-vitro* degradation rate. The GelMA hydrogels were placed in a small centrifuge tube containing 4 mL of 10 mM PBS, and then 50 μL of collagenase (10 U/mL) was added [36]. The weight of each hydrogel was weighed after removing excess water on the surface of the GelMA hydrogel with a filter paper at different time intervals. The degradation rate of GelMA hydrogel was calculated as following:

$$\text{Degradation (wt.-\%)} = \frac{W_1}{W_0} \times 100\% \quad (3)$$

In the formula above, the initial weight of GelMA hydrogel was recorded as W_0, the weight of the GelMA hydrogel after degradation was labeled as W_1. The weight of the samples was weighed every day.

2.6 Mechanical characterization

The GelMA hydrogel cylinders (diameter of 10 mm, thickness of 2 mm) with concentration of 7, 10, 15 and 30% were prepared. Young' modulus of the GelMA hydrogel was measured by the Instron universal testing machine after 24 h immersion in PBS. The compression speed was set as 0.1 mm/min, with three samples in each group.

2.7 Characterization of surface contact angle

The contact angles of the GelMA hydrogel were determined by sessile drop method. The samples were testing by using 1 μL of distilled water as medium on the digital microscope dino-light (Taiwan). Then angles were analyzed by Dino Capture 2 software.

2.8 Light transmittance

Optical transmittance is also an important factor to be considered for biomaterials used in corneal tissue engineering [37]. GelMA hydrogels were placed in PBS for 1 h and then the absorbance of the sample was obtained with a

Cytation5 Imaging Reader (BioTek Instruments, Winooski, VT, USA).

2.9 Cell evaluation

2.9.1 The adhesion, viability and morphology of cell

rBM-MSCs were provided by Procell Life Technology Co., Ltd. (Wuhan, China) and cultured in DMEM/F12 medium supplemented with 10% FBS and 1% penicillin/streptomycin. First, 7, 10, 15 or 30% rBM-MSCs-seeded GelMA hydrogels were prepared and cultured in DMEM/F12 supplemented with 10% FBS and 1% penicillin/streptomycin for 7 days in a 37 °C, 5% CO_2 incubator. The viability and adhesion of rBM-MSCs were confirmed by using live-dead assay kit. 4 μM calcein-AM was mixed in PBS to prepare the live staining solution and 4 μM propidium iodide was also mixed in PBS to prepare the dead staining solution. Then, the rBM-MSCs-seeded GelMA hydrogel was immersed in the live staining solution and incubated for 30 min, then transferred to the dead staining solution and incubated for 10 min. The images of GelMA hydrogel were taken by Cytation5 Imaging Reader. The ratio of the number of live cells to the total number of cells was calculated to obtain the viability of the rBM-MSCs on GelMA hydrogels by using ImageJ software. The adhesion rate was calculated by the ratio of the area of the green fluorescently stained cells to the total area by using ImageJ software. The morphology of rBM-MSCs was confirmed by phalloidin and DAPI staining. The stained samples were imaged using Cytation5 Imaging Reader.

2.9.2 Cell proliferation assay

The proliferation of rBM-MSCs on the GelMA hydrogels was examined with MTT assay. First, the rBM-MSCs-seeded GelMA hydrogels were cultured in 96-well plate, then incubated with 20 μL MTT for 4 h, after 1, 3, and 7 days. After removing the mixture, the DMSO solution was added and shook on a shaker for 10 min. Then the absorbance of supernatant was measured at 570 nm by Cytation5 Imaging Reader.

2.10 Differentiation of rBM-MSCs

Rat corneal keratocyte cells were provided by Procell Life Technology Co., Ltd. and cultured in DMEM supplemented with 0.1 mM/mL L-ascorbic-acid-2-phosphate and 2 mM/mL GlutaMAX^{TM} with the addition of 100 U/mL penicillin, 100 mg/mL streptomycin and 250 ng/mL amphotericin B. After three days, the medium was harvested and centrifuged. The supernatant was collected by 0.22 μm filter and used as keratocyte-conditioned medium

(KCM), which was directly transferred for the cultivation of rBM-MSCs [38].

Initially, rBM-MSCs-seeded GelMA hydrogel was cultured in complete DMEM/F12 medium for 24 h, and transferred to DMEM/F12 containing 10% KCM. Then the concentration of KCM in DMEM/F12 was gradually increased (10–50%). Because of the proliferation rate of rBM-MSCs decreased when the concentration of KCM was greater than 50%. The rBM-MSCs-seeded GelMA hydrogels were induced to differentiate for 14 days.

2.11 Quantitative RT-PCR

After rBM-MSCs were induced to differentiate for 2 weeks, total RNA was extracted with Trizol reagent. RNase-free water was used to dissolve the white RNA pellet, and the RNA concentration was measured with a spectrophotometer (NanoDrop OneC, Thermo Scientific). cDNA synthesis kit was used to synthesize the total cDNA. QRT-PCR was performed to detect the gene-specific of Keratocan, Lumican, Na^+,K^+-ATPase alpha 1 subunit (ALDH1A1), alpha-smooth muscle actin (α-SMA) and glyceraldehyde-3-phosphate dehydrogenase (GAPDH) using SYBR Premix Ex Taq. The CFX96^{TM} Real-time PCR (BioRad, Hercules, CA, USA) was used to quantify SybrGreen fluorescence of the amplified cDNA products. The results of the qRT-PCR were obtained by calculating the average expression of each target gene by using GAPDH as the reference gene. The primer sequences of the four different genes are shown in Table 1.

2.12 Immunofluorescent staining

The expression of Lumican in rBM-MSCs was detected by immunofluorescence staining, after rBM-MSCs were induced to differentiate for 2 weeks. The rBM-MSCs-seeded GelMA hydrogels were washed 3 times with PBS, then fixed with 4% paraformaldehyde (PFA) and permeabilized with 0.05% Triton X-100 to permeabilize fixed cells for 15 min. The rBM-MSCs-seeded GelMA hydrogels were incubated with a blocking agent (bovine serum albumin in PBS) for 30 min. Then the samples were incubated with anti-Lumican (diluted 1:250 in blocking reagent) at 4 °C overnight, then incubated with FITC-labeled goat anti-rabbit IgG (diluted 1:500 in a blocking agent) in dark for 2 h and DAPI for 10 min. The stained samples were imaged using Cytation5 Imaging Reader.

2.13 Statistical analysis

The experimental result data was analyzed by SPSS 20.0 and described in the form of mean $\pm$ standard deviation (SD). A one-way analysis of variance (ANOVA) was used to test whether there are differences between the data groups. $P < 0.05$ was considered statistically significant.

3 Results

3.1 Physical and chemical characterization

The infrared spectra of GelMA before and after photopolymerization is shown in Fig. 2. In the comparison between gelatin and GelMA, the new peak at 1533.51 cm^{-1} belonged to the N–H deformation vibration peak of the amide. The strong peak of C =O stretching vibration appeared at 1628.50 cm^{-1}. This is because the C=O on the amide was shifted from the acid anhydride. This indicated that the target GelMA was synthesized. As for the comparison between GelMA and GelMA hydrogel, after photopolymerization, the C=C stretching vibration

Table 1 Sequences of qRT-PCR primers

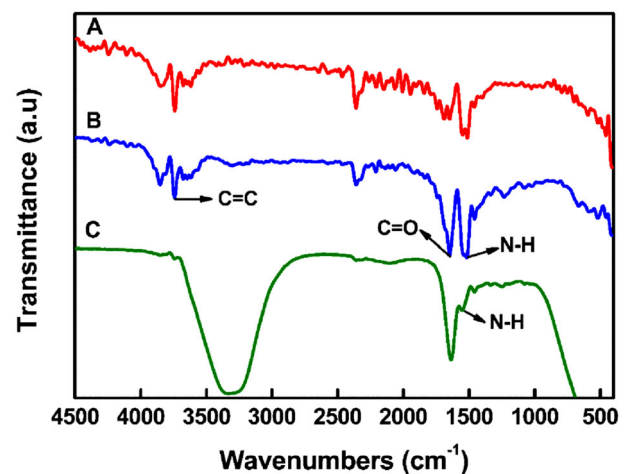| Genes	Primer sequence
Keratocan	Forward: 5′-TAGAGTACAGGACCCAGAGGAGTG-3′
	Reverse: 5′-GGGAAACTCGGTGGACAGAAGC-3′
Lumican	Forward: 5′-TCCGCTCCCAAAGTCCCTACAAG-3′
	Reverse: 5′-GCCTTTCAGAGAAGCCGAGACAG-3′
ALDH1A1	Forward: 5′-TCGTCAAGCCAGCAGAGCAAAC-3′
	Reverse: 5′-GACAATGGTCACCACGCCAGGAG-3′
α-SMA	Forward: 5′-GACCTCGTTTCTCCCTCCACCTC-3′
	Reverse: 5′-AGGCATCCAACACGGCAAGAAC-3′

Fig. 2 The infrared spectrum of GelMA before and after photopolymerization. **A** Gelatin, **B** GelMA [degree of MA modification (68%)] and **C** GelMA hydrogel

peak near 3769.13 cm^{-1} disappeared, while the C = O stretching vibration peak near 1628.50 cm^{-1} and the N–H stretching vibration peak near 1533.51 cm^{-1} were weakened. Judging from this, GelMA was polymerized under near-UV blue light ($\sim$ 405 nm) to form GelMA hydrogel.

The morphology of the GelMA hydrogel was detected by SEM, as shown in Fig. 3A-D. The inside of the GelMA hydrogel presented a three-dimensional porous structure, which affects the hydrophilicity and biological activity of the material. In order to measure the average pore size of the freeze-dried hydrogels, we used the Image J software. As shown in Fig. 3, the average pore size of 7%GelMA hydrogels was 183.45 $\pm$ 20.13 μm, 10%GelMA hydrogels was 93.61 $\pm$ 13.14 μm, 15%GelMA hydrogels was 50.78 $\pm$ 7.26 μm, and 30%GelMA hydrogels was 39.32 $\pm$ 9.25 μm. The results showed that the larger the concentration of GelMA, the smaller the pore size of the hydrogel. The porosity of the GelMA hydrogel is shown in the Fig. 3E. This indicated that the porosity of the hydrogel decreases with the increase of the concentration of GelMA. The porosity of 7%GelMA hydrogel was as high as 94.67 $\pm$ 1.71wt.-%.

3.2 Equilibrium water content and degradation performance

The corneal stroma contains approximately 78% water [39]. The equilibrium water content of 7, 10, 15 and 30% GelMA hydrogels is shown in Fig. 4A. The water content of hydrogels with different concentrations was significantly different. The equilibrium water contents of the 7%

(75 $\pm$ 3.14wt.-%) and 10% (71 $\pm$ 2.54wt.-%) GelMA hydrogels were comparable to that of the human cornea (78.0 $\pm$ 3.0wt.-%) [22]. When the concentration of GelMA increased, the equilibrium water content of the hydrogel decreased accordingly. With the increase of GelMA concentration, the interconnected GelMA network chains in the hydrogel were tightly packed to form a denser network structure. Meanwhile, the porosity of the hydrogel decreased, which reduced the swelling effect of water molecules on the hydrogel to a certain extent, resulting in a decrease in the equilibrium water content of the hydrogel [40].

The degradation of four concentrations of GelMA hydrogel in a 10 U/ml collagenase solution is shown in Fig. 4B. With the increase of concentration of GelMA, the degradation time of hydrogel in vitro was longer. Additionally, 7% of GelMA hydrogels were completely dissolved in collagenase within 3 days, 10% of GelMA hydrogels were dissolved within 5 days, 15% of GelMA hydrogels were dissolved within 7 days and 30% of GelMA hydrogels were dissolved within 11 days. The higher the concentration of GelMA hydrogel, the slower the degradation rate.

3.3 Mechanical characterization

The cornea responds to stress with both the elasticity of the biofilm and the viscosity of liquid as a soft tissue [41]. In order to study the mechanical properties of GelMA hydrogel, stress–strain curves were performed and recorded as shown in Fig. 4C. The strain changed linearly with
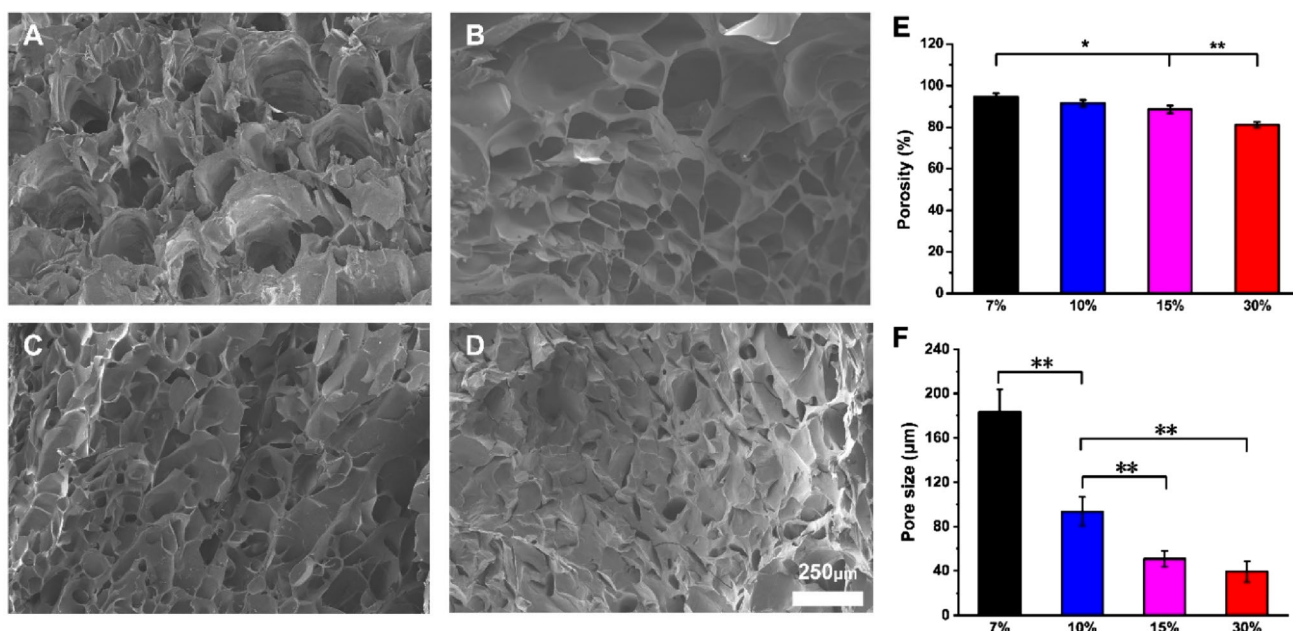

Fig. 3 The morphology (**A**: 7%; **B**: 10%; **C**: 15%; **D**: 30%), **E** porosity and **F** pore size of GelMA hydrogel
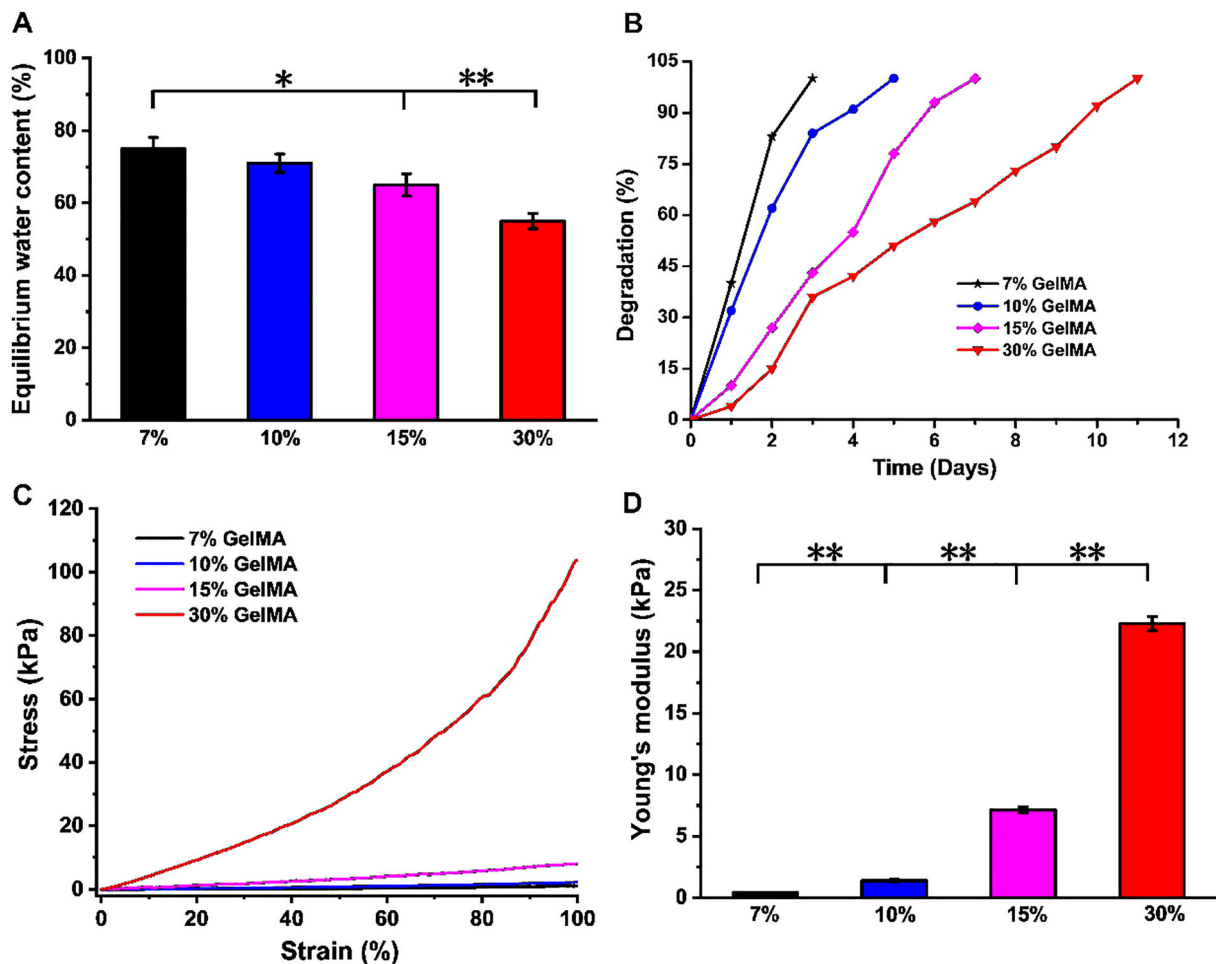
Fig. 4 **A** The equilibrium water content, **B** degradation performance, **C** stress–strain curve and **D** Young's modulus of GelMA hydrogel

the increase of stress. There was a little jitter on the curve, which represented the noise signal of the environment. The Young's modulus (Fig. 4D) of 7, 10, 15 and 30% GelMA hydrogels were 0.92 ± 0.85, 3.28 ± 1.17, 7.54 ± 0.94 and 30.12 ± 1.25 kPa, respectively. There were statistically significant differences ($p < 0.05$) among the groups. The mechanical properties of biomaterials have an important impact on the biological behaviors of the cells attached to or wrapped on them, including cell proliferation, differentiation, migration and adhesion [42]. For this reason, it is necessary to target the seeded cells (rBM-MSCs) to screen out the most suitable gel parameters for their three-dimensional growth [43].

3.4 Characterization of contact angle

The wettability of hydrogel surface depends on its chemical composition. The contact angles of GelMA hydrogels are shown in Fig. 5. The contact angles of 7, 10, 15 and 30% GelMA hydrogels were 37.36°, 50.24°, 64.12° and 73.89° after water staying on the GelMA hydrogel for 90 s,
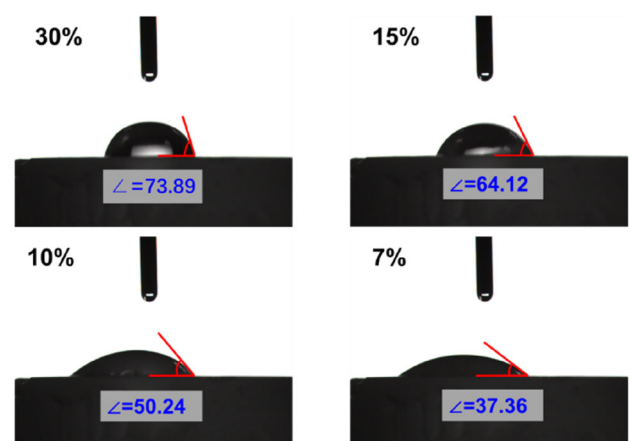

Fig. 5 Contact angles of GelMA hydrogels with different concentrations (7, 10, 15 and 30%)

respectively. It can be concluded that the hydrophilicity of the hydrogel was excellent, and 7% of GelMA hydrogel was the best.

3.5 Optical measurement-light transmittance

Figure 6 shows the transmittance curves of four GelMA hydrogels with different concentrations after immersing in PBS. The light transmittance of 7, 10, 15 and 30% GelMA hydrogels were about 87.53, 83.43, 76.72, and 66.35% at 400–800 nm, respectively. The results showed that the transparency of the hydrogel decreased with the increase of the concentration of GelMA hydrogel.

3.6 Cell evaluation

rBM-MSCs-seeded GelMA hydrogels were cultured at 37 °C, 5% CO_2 and the cell adhesion was examined 7 days later. As shown in Fig. 7A, green fluorescence represents live cells and red represents dead cells. The results showed that rBM-BMSCs had the best adhesion to the surface of 7% GelMA, with the most live cells. On the surface of 7, 10 and 15% GelMA, most of the cells were alive, while on 30% GelMA, there were relatively more dead cells. The survival and adhesion rates of rBM-MSCs cultured on GelMA hydrogel (7, 10, 15 or 30%) were compared (Fig. 7B, C). The survival rate of 7% GelMA was the highest, $94 \pm 4.67\%$. This result implied that rBM-MSCs had higher adhesion rate and activity under lower GelMA concentration.

The morphology of rBM-MSCs on GelMA hydrogels with different concentrations is shown in Fig. 8. It can be seen that the changes of GelMA concentration had no obvious effect on the cell morphology of rBM-MSCs.

rBM-MSCs-seeded GelMA hydrogel was cultivated and the proliferation of rBM-MSCs was judged by observing the absorbance at 1, 3, and 7 days (Fig. 9). The rBM-MSCs on the GelMA hydrogel of each concentration proliferated over time. The cell viability of hydrogels with different

concentrations was comparable at all time points. The proliferation of rBM-MSCs in 7% GelMA hydrogel was significantly different from that of in 15 and 30% GelMA hydrogels. However, on day 1, there was no significant difference in the proliferation of rBM-MSCs on the scaffold among different concentrations of hydrogels and there was significant difference in cell proliferation between 7% GelMA and 15%, 30% GelMA hydrogels on day 7. As the concentration of GelMA increased, cell viability decreased.

3.7 Expression of keratocyte markers in rBM-MSCs

The expression of keratocyte marker genes in rBM-MSCs including Keratocan, Lumican, ALDH1A1 and α-SMA was determined by qRT-PCR with 7% GelMA hydrogel group as the control group (Fig. 10). According to this figure, greater upregulated expression of Lumican and ALDH1A1 specific genes was observed in all four groups of rBM-MSCs-seeded hydrogel. The expression of Keratocan and α-SMA in the four groups of hydrogels was not significantly different. In addition, Lumican and ALDH1A1 expression levels were significantly increased in 30% GelMA hydrogel compared with other groups. These results suggested that 30% GelMA hydrogel can provide a better microenvironment for rBM-MSCs to successfully differentiate into keratocyte-like cells.

Furthermore, the immunofluorescence staining of Lumican of four different concentrations of hydrogels is shown in Fig. 11. According to the figure, the expression of Lumican was found in rBM-BMSCs induced to differentiate on the four different concentrations of hydrogels. However, rBM-MSCs showed a greater expression of Lumican on 30% GelMA hydrogel, which was significantly different from the other three groups.
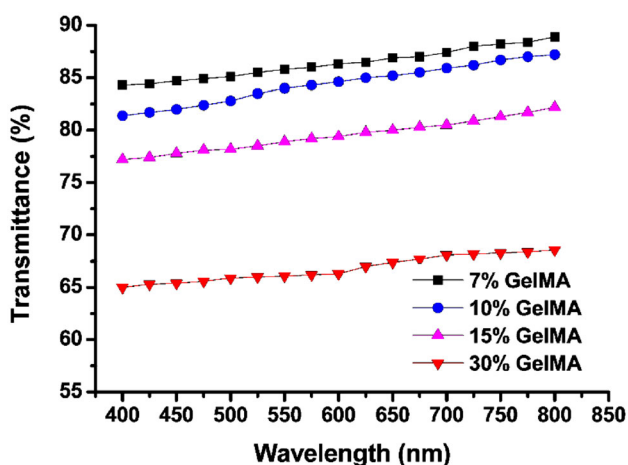
4 Discussion

The GelMA hydrogel used in this experiment is a natural biological scaffold with cell adhesion sites, matrix metalloenzymes (MMPs) response peptide sequences, photopolymerization and metabolizable properties. It is a kind of polymer reactant which is based on gelatin and chemically polymerized after adding MA [44, 45]. The principle of GelMA hydrogel photo-crosslinking is a covalent crosslinking reaction that relies on exposure to near-UV blue light (~ 405 nm) radiation to initiate a polymerization reaction of free radicals in the presence of a photoinitiator [46]. Gelatin solution has the characteristics of being able to physically crosslink at low temperature and the addition of MA group makes it have photosensitive characteristics, which can be quickly crosslinked under the condition of adding a suitable concentration of
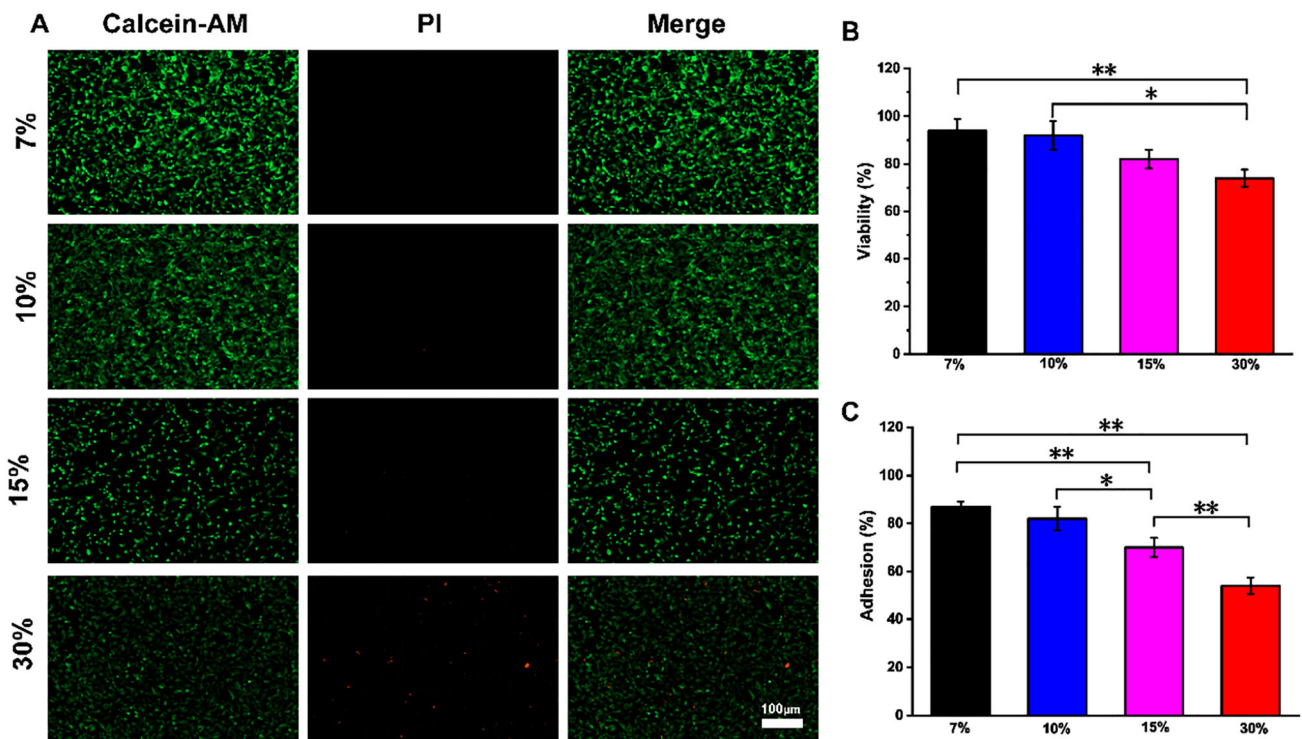

Fig. 6 The transmittance curves of four GelMA hydrogels with different concentrations when immersed in PBS

Fig. 7 The detection of cell adhesion and viability. **A** Live/dead staining shows the survival and adhesion of rBM-MSCs on GelMA hydrogel with different concentrations. Live cells: green (calcein-AM); Dead cells: red (PI). Scale bar: 100 μm. **B** The viability of rBM-MSCs on GelMA hydrogel. **C** The adhesion rate of rBM-MSCs on GelMA hydrogel
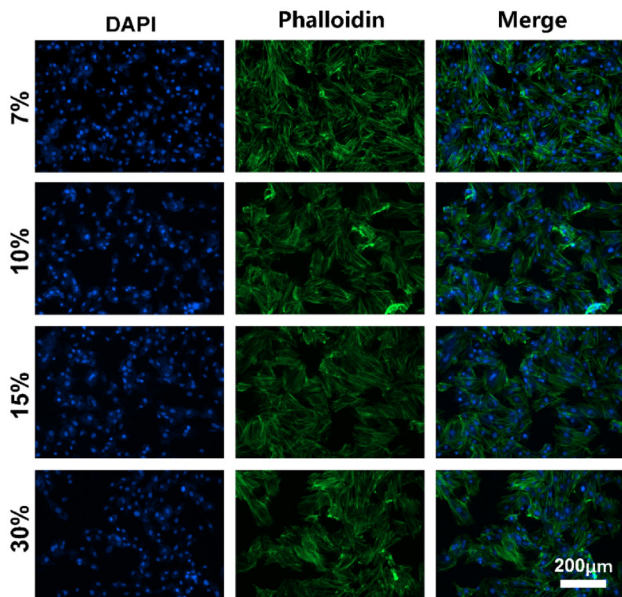

Fig. 8 Cell morphology of rBM-MSCs on GelMA hydrogel. Nucleus, blue (DAPI); f-actin, green (green fluorescently labeled phalloidin). Scale bar: 200 μm

Fig. 9 Proliferation of rBM-MSCs on GelMA hydrogels with different concentrations after 1, 3, 7 days of culture

photoinitiator and the crosslinking process has time and space adjustability. This indicates that the specific three-dimensional morphologi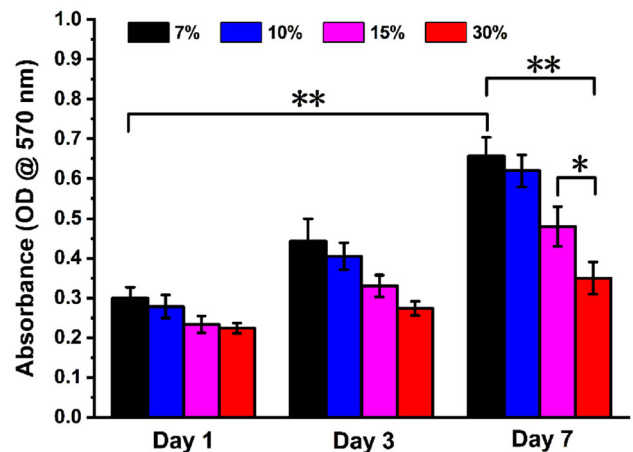cal structure of the gel can be modulated by means of microfluidics, which provides a good reference value and science for the regulation of cell behavior in basic research, cell-material interaction and tissue engineering organ reconstruction in clinical research background.

In this study, we prepared and characterized four different concentrations of GelMA hydrogel. As a carrier, GelMA hydrogel was transparent, biodegradable and suitable for the attachment and proliferation of rBM-MSCs. At
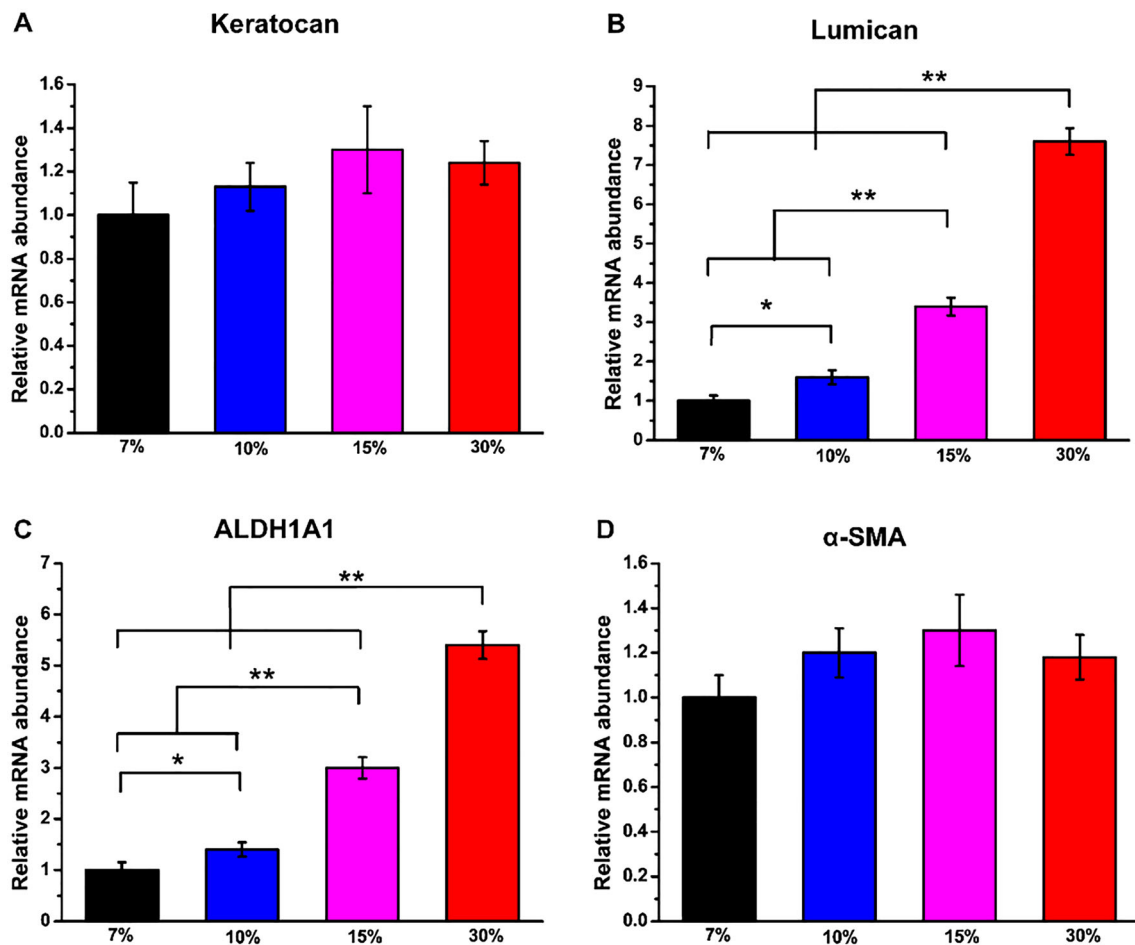
Fig. 10 qRT-PCR analysis of the expressions of keratocyte marker genes including **A** Keratocan, **B** Lumican, **C** ALDH1A1 and **D** α-SMA of rBM-MSCs cultured on GelMA hydrogel with different concentrations after 2 weeks of differentiation. The values are expressed as fold change and normalized to the GAPDH value ($n = 3$)

the same time, GelMA hydrogel was beneficial to induce the differentiation of rBM-MSCs. The results showed that higher concentration of GelMA hydrogel could promote the differentiation of rBM-MSCs into corneal keratocyte-like cells. These results demonstrated the potential of BM-MSCs in corneal tissue engineering.

The white foamy monomer of GelMA hydrogel can be scanned by a scanning electron microscope to show that the cross-section morphology of GelMA hydrogel biological scaffold was multi-pore and interconnected three-dimensional network structure. The three-dimensional porous structure can absorb nutrients in the culture medium and enable the antennae of the cells to grow inward along the micropores [47]. In addition, temperature will affect the pore size of the hydrogel. The temperature-sensitive hydrogel can adjust the water absorption of the hydrogel by changing the swelling temperature, so as to obtain a microporous structure with different pore sizes [48]. Different concentration of GelMA hydrogels had different crosslinking concentration and the greater the degree of

crosslinking, the smaller the degree of swelling. The results of the equilibrium water content showed that 7%GelMA hydrogel had the highest water content, which was similar to human normal cornea [27]. Degradation rate is an important factor to be considered in the implantation of hydrogels. Rapid degradation is not conducive to the growth of new tissues, so the appropriate degradation rate is conducive to the combination of hydrogel with surrounding tissues [19]. The compressive strength of human natural corneal stroma is 403–624 kPa [49]. The higher the concentration of GelMA, the better the mechanical properties of hydrogel. The young's modulus of 30%GelMA hydrogel was 30.12 ± 1.25 kPa, which was significantly different from that of natural cornea. However, the calculation of Young's modulus is also one of the main requirements of material research and further consideration should be given to improving the mechanical properties of hydrogels *in vivo*. The hydrophilicity or hydrophobicity of the surface of a biomaterial affects its interaction with cells. The stem cells attach and diffuse to a larger area on
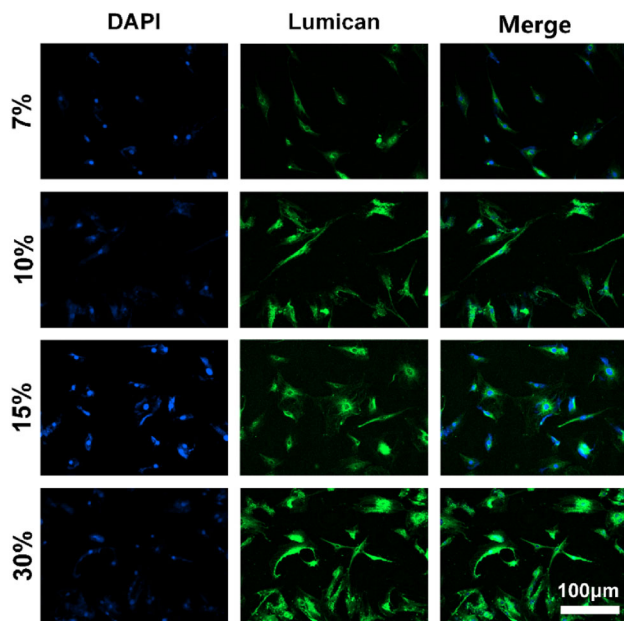
Fig. 11 The expression of Lumican in rBM-MSCs cultured on GelMA hydrogel with different concentrations was detected by immunofluorescence staining after 2 weeks. Nuclei, blue (DAPI); lumican, green. Scale bar: 100 μm

the surface of the material with better hydrophilicity and the cell proliferation is faster [50]. The light transmittance of normal corneal stroma is as high as 90% at 750 nm. Clinically, many reasons can cause corneal edema and turbidity. The light transmittance of diseased corneal tissue is about 30–80%. With the increase of corneal turbidity, corneal transmittance decreased sharply. The greater the concentration of GelMA, the lower the transmittance of the hydrogel. The light transmittance of 7%GelMA hydrogel was about 88.2% at 750 nm, which is close to human normal cornea [51]. In addition, the light transmittance of hydrogel increases with the increase of swelling time and after reaching the equilibrium of swelling, the light transmittance basically remains unchanged [19].

In the process of tissue repair and regeneration, stem cells play an important role. After proliferation and differentiation, stem cells can develop into mature cell lines with specific functions. BM-MSCs can be cultured *in vitro* and *in vivo* to induce differentiation into corneal epithelial cells, limbal epithelial cells and corneal stromal cells. BM-MSCs can differentiate into corneal epithelial cells after transplantation, effectively repair damaged corneal epithelial cell tissues, express a variety of cytokines, reduce inflammatory cell infiltration, reduce cell damage, inhibit cell apoptosis and reduce rejection after corneal transplantation [52, 53]. Yun et al. proved that BM-MSCs can significantly reduce corneal opacity. It was showed that

transplantation of allogeneic BM-MSCs is as safe and effective as transplantation of allogeneic limbal epithelial cells [54, 55]. Lumican protein is an extracellular protein, which is closely related to the normal development of the sclera, the maintenance of corneal transparency and the occurrence of myopia [56]. Keratocan is also important in maintaining corneal transparency. Corneal keratocytes express large amounts of corneal crystallin, a water-soluble protein such as ALDH1A1 that also helps to maintain corneal transparency. When corneal keratocytes proliferate continuously *in vitro* or corneal keratocytes were cultured with serum, they will differentiate into fibroblasts and myofibroblasts. These fibroblasts decrease the expression of corneal specific proteins and show up-regulated of α-SMA (mesenchymal marker) and down-regulated of Keratocan [38]. In this study, we found that 7%GelMA hydrogel could promote the growth and proliferation of rBM-MSCs, while 30%GelMA hydrogel has a low cell adhesion rate. This may be because the 7%GelMA hydrogel has larger internal pore size and higher porosity, which is conducive to the transport of nutrients and the discharge of metabolites. In Shin et al. 's study, reduced graphene oxide (rGO)-GelMA (7% w/v) hydrogel could promote the growth and proliferation of cells [57]. However, 30%GelMA hydrogel had small internal pore size and low porosity, which is not conducive to the growth of rBM-MSCs [58]. In addition, it may be that high concentrations of GelMA hydrogels contain less RGD, which is the main binding site for cells. It exists in a variety of extracellular matrices and can effectively promote the adhesion of cells to biomaterials. At the same time, we found that the expression level of Lumican and ALDH1A1 was the highest in the rBM-MSCs seeded on 30%GelMA hydrogel.

Mechanobiology studies have shown that the differentiation of limbal stem cells is controlled by changes in the hardness of the underlying matrix. The harder matrix promotes differentiation, but the softer matrix does not [59]. In our study, 30%GelMA hydrogel with better mechanical strength can better promote the expression of corneal keratocytes marker genes in rBM-MSCs, which is consistent with their study. According to previous reports, tissue biomechanics are important for maintaining the homeostasis of the stromal layer of the cornea, highlighting the close interaction between the corneal cells and the underlying supporting matrix [60]. Therefore, the ideal biomaterial for corneal stroma tissue engineering should mimic the unique biomechanical properties of the extracellular matrix of the cornea [61]. Corneal stromal hardness is determined by the number and density of proteins present in the extracellular matrix, such as collagen, fibrin and proteoglycan. Yet their cross-linking and their spatial orientation are difficult to recreate in a laboratory setting. So

this is also an important direction of future corneal stroma tissue engineering research [62].

In this study, the physicochemical and biological properties of GelMA hydrogels in different concentrations (7%, 10%, 15%, 30%) were evaluated. Our results showed that 7%GelMA hydrogel had higher water content and porosity, better optical properties and hydrophilicity. In addition, it was more beneficial to the growth and proliferation of rBM-MSCs. However, the 30%GelMA hydrogel had the best mechanical properties and could promote the differentiation of rBM-MSCs into keratocyte-like cells. This study laid a theoretical and experimental basis for further tissue engineered corneal stroma transplantation and provided a new idea for the source of seed cells of corneal tissue engineering. A single material may not be able to meet the various characteristics of corneal stroma tissue, so composite biomaterials are our future research direction.

Declaration

Conflict of interest The authors have no financial conflicts of interest.

Ethical statement There are no animal experiments carried out for this article.

References

1. Duan X, Sheardown H. Dendrimer crosslinked collagen as a corneal tissue engineering scaffold: mechanical properties and corneal epithelial cell interactions. Biomaterials. 2006;27:4608–17.
2. Vrana NE, Builles N, Kocak H, Gulay P, Justin V, Malbouyres M, et al. EDC/NHS cross-linked collagen foams as scaffolds for artificial corneal stroma. J Biomater Sci Polym Ed. 2007;18:1527–45.
3. Cao D, Zhang Y, Cui Z, Du Y, Shi Z. New strategy for design and fabrication of polymer hydrogel with tunable porosity as artificial corneal skirt. Mater Sci Eng C Mater Biol Appl. 2017;70:665–72.
4. Islam MM, Buznyk O, Reddy JC, Pasyechnikova N, Alarcon EI, Hayes S, et al. Biomaterials-enabled cornea regeneration in patients at high risk for rejection of donor tissue transplantation. NPJ Regen Med. 2018;3:2.
5. Chen F, Le P, Fernandes-Cunha GM, Heilshorn SC, Myung D. Bio-orthogonally crosslinked hyaluronate-collagen hydrogel for suture-free corneal defect repair. Biomaterials. 2020;255:120176.
6. Karamichos D. Ocular tissue engineering: current and future directions. J Funct Biomater. 2015;6:77–80.
7. Feiz V, Mannis MJ, Kandavel G, McCarthy M, Izquierdo L, Eckert M, et al. Surface keratopathy after penetrating keratoplasty. Trans Am Ophthalmol Soc. 2001;99:159–68.
8. Reinhart WJ, Musch DC, Jacobs DS, Lee WB, Kaufman SC, Shtein RM. Deep anterior lamellar keratoplasty as an alternative to penetrating keratoplasty a report by the american academy of ophthalmology. Ophthalmology. 2011;118:209–18.
9. Jirásková N, Rozsival P, Burova M, Kalfertova M. AlphaCor artificial cornea: clinical outcome. Eye (Lond). 2011;25:1138–46.
10. Ruberti JW, Zieske JD. Prelude to corneal tissue engineering—gaining control of collagen organization. Prog Retin Eye Res. 2008;27:549–77.
11. Mahdavi SS, Abdekhodaie MJ, Mashayekhan S, Baradaran-Rafii A, Djalilian AR. Bioengineering approaches for corneal regenerative medicine. Tissue Eng Regen Med. 2020;17:567–93.
12. Barabadi Z, Azami M, Sharifi E, Karimi R, Lotfibakhshaiesh N, Roozafzoon R, et al. Fabrication of hydrogel based nanocomposite scaffold containing bioactive glass nanoparticles for myocardial tissue engineering. Mater Sci Eng C Mater Biol Appl. 2016;69:1137–46.
13. Yang CY, Song B, Ao Y, Nowak AP, Abelowitz RB, Korsak RA, et al. Biocompatibility of amphiphilic diblock copolypeptide hydrogels in the central nervous system. Biomaterials. 2009;30:2881–98.
14. Recouvreux DO, Rambo CR, Berti FV, Carminatti CA, Antônio RV, Porto LM. Novel three-dimensional cocoon-like hydrogels for soft tissue regeneration. Mater Sci Eng C Mater Biol Appl. 2011;31:151–7.
15. Wright B, Mi S, Connon CJ. Towards the use of hydrogels in the treatment of limbal stem cell deficiency. Drug Discov Today. 2013;18:79–86.
16. Niu G, Choi JS, Wang Z, Skardal A, Giegengack M, Soker S. Heparin-modified gelatin scaffolds for human corneal endothelial cell transplantation. Biomaterials. 2014;35:4005–14.
17. Hayes S, Lewis P, Islam MM, Doutch J, Sorensen T, White T, et al. The structural and optical properties of type III human collagen biosynthetic corneal substitutes. Acta Biomater. 2015;25:121–30.
18. Lawrence BD, Marchant JK, Pindrus MA, Omenetto FG, Kaplan DL. Silk film biomaterials for cornea tissue engineering. Biomaterials. 2009;30:1299–308.
19. Goodarzi H, Jadidi K, Pourmotabed S, Sharifi E, Aghamollaei H. Preparation and in vitro characterization of cross-linked collagen-gelatin hydrogel using EDC/NHS for corneal tissue engineering applications. Int J Biol Macromol. 2019;126:620–32.
20. Stafiej P, Küng F, Thieme D, Czugala M, Kruse FE, Schubert DW, et al. Adhesion and metabolic activity of human corneal cells on PCL based nanofiber matrices. Mater Sci Eng C Mater Biol Appl. 2017;71:764–70.
21. Yoeruek E, Bayyoud T, Maurus C, Hofmann J, Spitzer MS, Bartz-Schmidt KU, et al. Decellularization of porcine corneas and repopulation with human corneal cells for tissue-engineered xenografts. Acta Ophthalmol. 2012;90:e125–31.
22. Liu Y, Ren L, Wang Y. Crosslinked collagen-gelatin-hyaluronic acid biomimetic film for cornea tissue engineering applications. Mater Sci Eng C Mater Biol Appl. 2013;33:196–201.
23. Galis ZS, Khatri JJ. Matrix metalloproteinases in vascular remodeling and atherogenesis: the good, the bad, and the ugly. Circ Res. 2002;90:251–62.
24. Nichol JW, Koshy ST, Bae H, Hwang CM, Yamanlar S, Khademhosseini A. Cell-laden microengineered gelatin methacrylate hydrogels. Biomaterials. 2010;31:5536–44.
25. Shim K, Kim SH, Lee D, Kim B, Kim TH, Jung Y, et al. Fabrication of micrometer-scale porous gelatin scaffolds for 3D cell culture. J Ind Eng Chem. 2017;50:183–9.

26. Chen MB, Srigunapalan S, Wheeler AR, Simmons CA. A 3D microfluidic platform incorporating methacrylated gelatin hydrogels to study physiological cardiovascular cell-cell interactions. Lab Chip. 2013;13:2591–8.

27. Farasatkia A, Kharaziha M, Ashrafizadeh F, Salehi S. Transparent silk/gelatin methacrylate (GelMA) fibrillar film for corneal regeneration. Mater Sci Eng C Mater Biol Appl. 2021;120:111744.

28. Kilic Bektas C, Hasirci V. Cell loaded GelMA: HEMA IPN hydrogels for corneal stroma engineering. J Mater Sci Mater Med. 2019;31:2.

29. Venugopal B, Mohan S, Kumary TV, Anil Kumar PR. Peripheral blood as a source of stem cells for regenerative medicine: emphasis towards corneal epithelial reconstruction-an in vitro study. Tissue Eng Regen Med. 2020;17:495–510.

30. Carter K, Lee HJ, Na KS, Fernandes-Cunha GM, Blanco IJ, Djalilian A, et al. Characterizing the impact of 2D and 3D culture conditions on the therapeutic effects of human mesenchymal stem cell secretome on corneal wound healing in vitro and ex vivo. Acta Biomater. 2019;99:247–57.

31. Demirayak B, Yüksel N, Çelik OS, Subaşı C, Duruksu G, Unal ZS, et al. Effect of bone marrow and adipose tissue-derived mesenchymal stem cells on the natural course of corneal scarring after penetrating injury. Exp Eye Res. 2016;151:227–35.

32. Zakirova EY, Valeeva AN, Aimaletdinov AM, Nefedovskaya LV, Akhmetshin RF, Rutland CS, et al. Potential therapeutic application of mesenchymal stem cells in ophthalmology. Exp Eye Res. 2019;189:107863.

33. Rohaina CM, Then KY, Ng AM, Wan Abdul Halim WH, Zahidin AZ, Saim A, et al. Reconstruction of limbal stem cell deficient corneal surface with induced human bone marrow mesenchymal stem cells on amniotic membrane. Transl Res. 2014;163:200–10.

34. Van Den Bulcke AI, Bogdanov B, De Rooze N, Schacht EH, Cornelissen M, Berghmans H. Structural and rheological properties of methacrylamide modified gelatin hydrogels. Biomacromolecules. 2000;1:31–8.

35. Liu W, Deng C, McLaughlin CR, Fagerholm P, Lagali NS, Heyne B, et al. Collagen-phosphorylcholine interpenetrating network hydrogels as corneal substitutes. Biomaterials. 2009;30:1551–9.

36. He Y, Hou Z, Wang J, Wang Z, Li X, Liu J, et al. Assessment of biological properties of recombinant collagen-hyaluronic acid composite scaffolds. Int J Biol Macromol. 2020;149:1275–84.

37. Rizwan M, Peh GSL, Ang HP, Lwin NC, Adnan K, Mehta JS, et al. Sequentially-crosslinked bioactive hydrogels as nano-patterned substrates with customizable stiffness and degradation for corneal tissue engineering applications. Biomaterials. 2017;120:139–54.

38. Park SH, Kim KW, Chun YS, Kim JC. Human mesenchymal stem cells differentiate into keratocyte-like cells in keratocyte-conditioned medium. Exp Eye Res. 2012;101:16–26.

39. Sharifi E, Azami M, Kajbafzadeh AM, Moztarzadeh F, Faridi-Majidi R, Shamousi A, et al. Preparation of a biomimetic composite scaffold from gelatin/collagen and bioactive glass fibers for bone tissue engineering. Mater Sci Eng C Mater Biol Appl. 2016;59:533–41.

40. Du YA, Lo E, Ali S, Khademhosseini A. Directed assembly of cell-laden microgels for fabrication of 3D tissue constructs. Proc Natl Acad Sci U S A. 2008;105:9522–7.

41. Elsheikh A, Geraghty B, Rama P, Campanelli M, Meek KM. Characterization of age-related variation in corneal biomechanical properties. J R Soc Interface. 2010;7:1475–85.

42. Garcia-Porta N, Fernandes P, Queiros A, Salgado-Borges J, Parafita-Mato M, González-Méijome JM. Corneal biomechanical properties in different ocular conditions and new measurement techniques. ISRN Ophthalmol. 2014;2014:724546.

43. Luo LJ, Lai JY, Chou SF, Hsueh YJ, Ma DH. Development of gelatin/ascorbic acid cryogels for potential use in corneal stromal tissue engineering. Acta Biomater. 2018;65:123–36.

44. Arica TA, Guzelgulgen M, Yildiz AA, Demir MM. Electrospun GelMA fibers and p(HEMA) matrix composite for corneal tissue engineering. Mater Sci Eng C Mater Biol Appl. 2021;120:111720.

45. Sun M, Sun X, Wang Z, Guo S, Yu G, Yang H. Synthesis and properties of gelatin methacryloyl (GelMA) hydrogels and their recent applications in load-bearing tissue. Polymers (Basel). 2018;10:1290.

46. Dragusin DM, Van Vlierberghe S, Dubruel P, Dierick M, Van Hoorebeke L, Declercq HA, et al. Novel gelatin-PHEMA porous scaffolds for tissue engineering applications. Soft Matter. 2012;8:9589–602.

47. Yue K, Trujillo-de Santiago G, Alvarez MM, Tamayol A, Annabi N, Khademhosseini A. Synthesis, properties, and biomedical applications of gelatin methacryloyl (GelMA) hydrogels. Biomaterials. 2015;73:254–71.

48. Aldana AA, Rial-Hermida MI, Abraham GA, Concheiro A, Alvarez-Lorenzo C. Temperature-sensitive biocompatible IPN hydrogels based on poly (NIPA-PEGdma) and photocrosslinkable gelatin methacrylate. Soft Mater. 2017;15:341–9.

49. Ma J, Wang Y, Wei P, Jhanji V. Biomechanics and structure of the cornea: implications and association with corneal disorders. Surv Ophthalmol. 2018;63:851–61.

50. Shin YN, Kim BS, Ahn HH, Lee JH, Kim KS, Lee JY, et al. Adhesion comparison of human bone marrow stem cells on a gradient wettable surface prepared by corona treatment. Appl Surf Sci. 2008;255:293–6.

51. Meek KM, Knupp C. Corneal structure and transparency. Prog Retin Eye Res. 2015;49:1–16.

52. Choong PF, Mok PL, Cheong SK, Then KY. Mesenchymal stromal cell-like characteristics of corneal keratocytes. Cytotherapy. 2007;9:252–8.

53. Espana EM, He H, Kawakita T, Di Pascuale MA, Raju VK, Liu CY, et al. Human keratocytes cultured on amniotic membrane stroma preserve morphology and express keratocan. Invest Ophthalmol Vis Sci. 2003;44:5136–41.

54. Calonge M, Pérez I, Galindo S, Nieto-Miguel T, López-Paniagua M, Fernández I, et al. A proof-of-concept clinical trial using mesenchymal stem cells for the treatment of corneal epithelial stem cell deficiency. Transl Res. 2019;206:18–40.

55. Yun YI, Park S, Lee HJ, Ko JH, Kim MK, Wee WR, et al. Comparison of the anti-inflammatory effects of induced pluripotent stem cell-derived and bone marrow-derived mesenchymal stromal cells in a murine model of corneal injury. Cytotherapy. 2017;19:28–35.

56. Chen J, Wong-Chong J, SundarRaj N. FGF-2-and TGF-beta 1-induced downregulation of Lumican and Keratocan in activated corneal keratocytes by JNK signaling pathway. Invest Ophthalmol Vis Sci. 2011;52:8957–64.

57. Shin SR, Zihlmann C, Akbari M, Assawes P, Cheung L, Zhang K, et al. Reduced graphene oxide-GelMA hybrid hydrogels as scaffolds for cardiac tissue engineering. Small. 2016;12:3677–89.

58. Kwak BS, Choi W, Jeon JW, Won JI, Sung GY, Kim B, et al. In vitro 3D skin model using gelatin methacrylate hydrogel. J Ind Eng Chem. 2018;66:254–61.

59. Chen J, Backman LJ, Zhang W, Ling C, Danielson P. Regulation of keratocyte phenotype and cell behavior by substrate stiffness. ACS Biomater Sci Eng. 2020;6:5162–71.

60. Zakirova EY, Valeeva AN, Aimaletdinov AM, Nefedovskaya LV, Akhmetshin RF, Rutland CS, et al. Potential therapeutic application of mesenchymal stem cells in ophthalmology. Exp Eye Res. 2019;189:107863.

61. Hong H, Kim H, Han SJ, Jang J, Kim HK, Cho DW, et al. Compressed collagen intermixed with cornea-derived decellularized extracellular matrix providing mechanical and biochemical niches for corneal stroma analogue. Mater Sci Eng C Mater Biol Appl. 2019;103:109837.

62. Urbanczyk M, Layland SL, Schenke-Layland K. The role of extracellular matrix in biomechanics and its impact on bioengineering of cells and 3D tissues. Matrix Biol. 2020;85–86:1–14.

Publisher's Note Springer Nature remains neutral with regard to jurisdictional claims in published maps and institutional affiliations.